

Study of the process $e^+e^- \rightarrow \omega\eta\pi^0$ in the energy range $\sqrt{s} < 2$ GeV with the SND detector

M. N. Achasov,^{1,2} V. M. Aulchenko,^{1,2} A. Yu. Barnyakov,^{1,2} K. I. Beloborodov,^{1,2} A. V. Berdyugin,^{1,2,*}
 D. E. Berkaev,^{1,2} A. G. Bogdanchikov,¹ A. A. Botov,¹ T. V. Dimova,^{1,2} V. P. Druzhinin,^{1,2}
 V. B. Golubev,^{1,2} L. V. Kardapoltsev,^{1,2} A. G. Kharlamov,^{1,2} I. A. Koop,^{1,2,3} A. A. Korol,^{1,2}
 D. P. Kovrizhin,^{1,2} S. V. Koshuba,¹ A. S. Kupich,¹ A. P. Lysenko,¹ N. A. Melnikova,¹ K. A. Martin,¹
 E. V. Pakhtusova,¹ A. E. Obrazovsky,¹ E. A. Perevedentsev,^{1,2} Yu. A. Rogovsky,^{1,2} S. I. Serednyakov,^{1,2}
 Z. K. Silagadze,^{1,2} Yu. M. Shatunov,^{1,2} P. Yu. Shatunov,^{1,2} D. A. Shtol,^{1,2} A. N. Skrinsky,¹
 I. K. Surin,^{1,2} Yu. A. Tikhonov,^{1,2} Yu. V. Usov,^{1,2} A. V. Vasiljev,^{1,2} and I. M. Zemlyansky^{1,2}

¹*Budker Institute of Nuclear Physics, SB RAS, Novosibirsk, 630090, Russia*

²*Novosibirsk State University, Novosibirsk, 630090, Russia*

³*Novosibirsk State Technical University, Novosibirsk, 630092, Russia*

The process $e^+e^- \rightarrow \omega\eta\pi^0$ is studied in the energy range 1.45 – 2.00 GeV using data with an integrated luminosity of 33 pb⁻¹ accumulated by the SND detector at the e^+e^- collider VEPP-2000. The $e^+e^- \rightarrow \omega\eta\pi^0$ cross section is measured for the first time. The cross section has a threshold near 1.75 GeV. Its value is about 2 nb in the energy range 1.8–2.0 GeV. The dominant intermediate state for the process $e^+e^- \rightarrow \omega\eta\pi^0$ is found to be $\omega a_0(980)$.

PACS numbers: 13.66.Bc 14.40.Be 13.40.Gp 12.40.Vv

I. INTRODUCTION

This work continues the study of multiphoton processes $e^+e^- \rightarrow n\gamma$ in the center-of-mass (c.m.) energy domain $\sqrt{s} < 2$ GeV with the SND detector [1–4]. The main goal of these studies is the measurement of radiative decays of excited vector resonances of the ρ , ω and ϕ families [2], as well as the search for rare processes of C -even resonance production in the e^+e^- annihilation [3, 4]. While searching for the rare reactions mentioned above, hadronic processes containing ω -meson in the final state decaying into $\pi^0\gamma$ constitute a significant background (the $\omega \rightarrow \pi^0\gamma$ branching fraction is $(8.28 \pm 0.28)\%$ [5]). For example, the process $e^+e^- \rightarrow \omega\pi^0 \rightarrow \pi^0\pi^0\gamma$ [1] dominates in the five-photon final state and hinders the search for the radiative processes $e^+e^- \rightarrow f_0\gamma, f_2\gamma$.

The $e^+e^- \rightarrow \eta\pi^0\pi^0\gamma$ process studied in this work is important to search for the radiative processes $e^+e^- \rightarrow \eta'\gamma$ and $f_1(1285)\gamma$. A possible source of hadronic background in the $\eta\pi^0\pi^0\gamma$ final state is the process $e^+e^- \rightarrow \omega\eta\pi^0$.

At energies below 2 GeV, the total cross section of e^+e^- annihilation into hadrons needed, for example, to calculate the running coupling constant of the electromagnetic interactions, is determined as a sum of exclusive hadronic cross sections. The process $e^+e^- \rightarrow \omega\eta\pi^0$ has not previously been measured and was not included in this sum. In this work we select this process for the first time and measure its cross section.

II. DETECTOR AND EXPERIMENT

The SND detector collects data at the e^+e^- collider VEPP-2000 [6] operating at c.m. energies $\sqrt{s} = 0.3 - 2.0$ GeV. This analysis uses data collected in 2010-2012. During the experiments, the energy range 1.05-2.00 GeV was scanned several times with a step of 20-25 MeV. Because of the smallness of statistics, we measure the cross section averaged over the energy intervals, listed in Table I.

A detailed description of the SND detector is given in Refs. [7–10]. The main part of this non-magnetic detector is a three-layer spherical electromagnetic calorimeter based on NaI(Tl) crystals. The solid angle coverage of the calorimeter is 95% of 4π . Its energy resolution for photons is $\sigma_{E_\gamma}/E_\gamma = 4.2\%/\sqrt[4]{E_\gamma(\text{GeV})}$, and the angular resolution is about 1.5° . Direction of charged particles are measured in a tracking system consisting of a nine-layer drift chamber and a proportional chamber with the signal readout from the cathode strips. The solid angle coverage of the tracking

*e-mail:berdugin@inp.nsk.su

system is 94% of 4π . From the outside the SND calorimeter is surrounded by a muon system. In this analysis, the muon system veto is used to suppress the cosmic-ray background.

Simulation of the signal and background processes is performed using Monte-Carlo generators that take into account initial-state radiative corrections calculated according to Ref. [11]. In particular, emission of an additional photon is simulated with the angular distribution according to Ref [12]. Interactions of the particles produced in the e^+e^- annihilation with the detector material are modeled using the GEANT4 package [13]. Simulation takes into account changes in the experimental conditions during the data taking, in particular, dead detector channels and variations of the beam-induced background. The beam background leads to the appearance of spurious photons and charged tracks in data events. To account for this effect in the simulation, special background events, recorded during the experiment with a random trigger, are used. Fired detector channels in these events are superimposed on the simulated events.

In this work, the $e^+e^- \rightarrow \omega\eta\pi^0$ process is studied in the channel $e^+e^- \rightarrow \eta\pi^0\pi^0\gamma \rightarrow 7\gamma$. Since the final state for the process under study contains no charged particles, we use the process $e^+e^- \rightarrow \gamma\gamma$ for normalization. As a result of the normalization a part of systematic uncertainties associated with the hardware event selection and spurious charged tracks from the beam background are canceled out. Accuracy of the luminosity measurement using the $e^+e^- \rightarrow \gamma\gamma$ process is 2.2% [1].

III. SELECTION CRITERIA

The selection of signal $e^+e^- \rightarrow \eta\pi^0\pi^0\gamma \rightarrow 7\gamma$ events is performed in two stages. Initially, events with exactly 7 photons with energy greater than 20 MeV, no charged particles, and for which the muon-system veto is not triggered, are selected. For these events, the following conditions on the total energy deposition in the calorimeter E_{EMC} and on the total event momentum P_{EMC} , calculated using energy depositions in calorimeter crystals, are imposed:

$$0.7 < E_{\text{EMC}}/\sqrt{s} < 1.2, \quad P_{\text{EMC}}/\sqrt{s} < 0.3, \quad (E_{\text{EMC}} - P_{\text{EMC}})/\sqrt{s} > 0.7. \quad (1)$$

The transverse profile of the energy deposition in the calorimeter for reconstructed photons is required to be consistent with that expected for an electromagnetic shower [14]. The latter requirement provides separation of events with well isolated photons from those with merged photons or with clusters in the calorimeter produced by K_L mesons.

The main background processes are the following: $e^+e^- \rightarrow \omega\pi^0 \rightarrow \pi^0\pi^0\gamma$, $e^+e^- \rightarrow \omega\pi^0\pi^0, \eta\gamma \rightarrow \pi^0\pi^0\pi^0\gamma$, $e^+e^- \rightarrow \omega\eta \rightarrow \eta\pi^0\gamma$ and $e^+e^- \rightarrow K_S K_L \pi^0$ with the decay $K_S \rightarrow \pi^0\pi^0$. The process $e^+e^- \rightarrow \pi^0\pi^0\gamma$, having five photons in the final state, is a background source because of a relatively large cross section. Additional photons in $e^+e^- \rightarrow \pi^0\pi^0\gamma$ events arise from splitting of electromagnetic showers, initial state radiation, and beam-induced background.

Further selection of events is based on kinematic fits, which use the measured photon angles and energies as input parameters. The fit is performed under the hypothesis that the seven-photon event proceed through the particular set of intermediate particles (with corresponding mass constraints), and satisfies energy-momentum conservation laws. As a result of the kinematic fit, photon energies are refined and the χ^2 of the assumed kinematic hypothesis is calculated. First of all, the $e^+e^- \rightarrow 7\gamma$ hypothesis is tested, and the condition $\chi_{7\gamma}^2 < 30$ is imposed. Then the photon pairs, candidates for the π^0 and η mesons, are searched. It is required that the invariant mass of the candidate is in the range $(m_{\pi^0, \eta} - 50 \text{ MeV}, m_{\pi^0, \eta} + 50 \text{ MeV})$. Events with one η meson candidate and two π^0 candidates are selected as possible signal events. To suppress the background from the processes $e^+e^- \rightarrow \omega\pi^0\pi^0, \eta\gamma \rightarrow \pi^0\pi^0\pi^0\gamma$, events containing three π^0 candidates are rejected. A kinematic fit is also performed to the $e^+e^- \rightarrow \pi^0\pi^0\gamma$ hypothesis. All five-photon combinations with two π^0 -meson candidates are tested. Events with $\chi_{\pi^0\pi^0\gamma}^2 < 50$ are rejected. For remaining events, a kinematic fit is performed to the $e^+e^- \rightarrow \eta 2\pi^0\gamma$ hypothesis. The $\chi_{\eta 2\pi^0\gamma}^2$ distributions for data and simulated $e^+e^- \rightarrow \eta 2\pi^0\gamma$ events are shown in Figure 1. Figure 2 shows the distributions of the two-photon invariant mass for π^0 and η meson candidates for selected data and simulated $e^+e^- \rightarrow \eta 2\pi^0\gamma$ events. It is evident from the distributions in Figs. 1 and 2 that most selected events arise from the process $e^+e^- \rightarrow \eta 2\pi^0\gamma$.

Figure 3 shows the distribution of the $\pi^0\gamma$ invariant mass ($M_{\pi^0\gamma}$) for 106 $e^+e^- \rightarrow \eta 2\pi^0\gamma$ candidate events. The calculated background from the processes listed above is 9.2 events (3 events from $\omega\eta$, 3 events from $\omega\pi^0\pi^0$, 2 events from $K_S K_L \pi^0$, 1 event from $\eta\gamma$). To calculate the cross sections of these background processes, we use the results of Refs. [2, 15–17] and isotopic relations.

The histogram in Fig. 3 shows the simulated distribution for the sum of the signal and estimated background under the assumption that the signal is from the process $e^+e^- \rightarrow \omega\eta\pi^0$. The simulated distribution is normalized to the number of selected data events. It is seen that at the existing statistical level these two contributions are sufficient to describe the distribution of selected $e^+e^- \rightarrow \eta 2\pi^0\gamma$ candidate events.

For the final selection of $e^+e^- \rightarrow \omega\eta\pi^0$ events, the condition $|M_{\pi^0\gamma} - M_\omega| < 50 \text{ MeV}$ is required for at least one $\pi^0\gamma$ combination in an event. This condition is satisfied by 62 events. Their distribution over the energy intervals is given

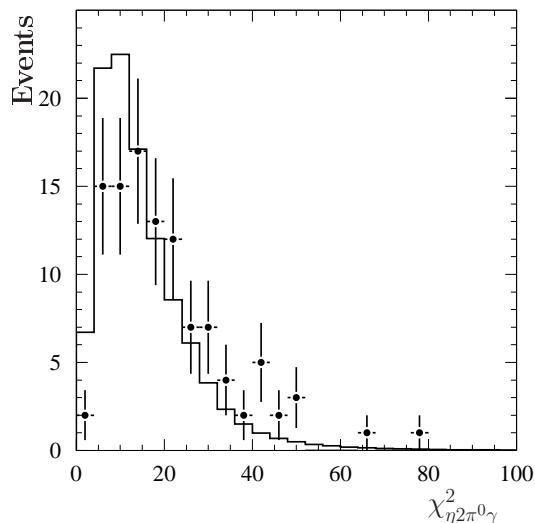


FIG. 1: The $\chi_{\eta 2\pi^0\gamma}^2$ distributions for selected data events (points with error bars) and for simulated $e^+e^- \rightarrow \eta 2\pi^0\gamma$ events (histogram).

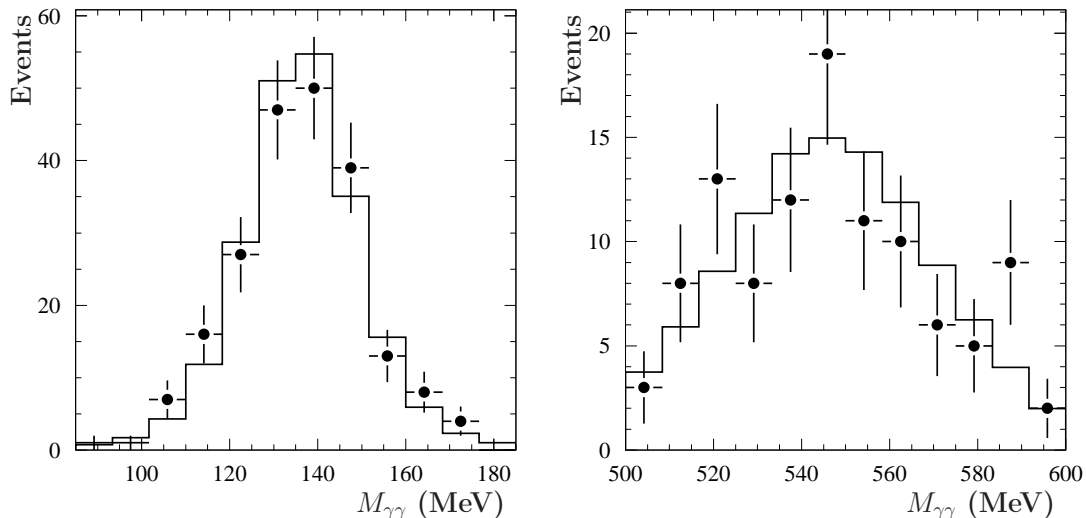


FIG. 2: The distributions of the two-photon invariant mass of π^0 -meson candidates (left, two entries per events) and of η -meson candidates (right) for selected data events (points with error bars) and for simulated $e^+e^- \rightarrow \eta 2\pi^0\gamma$ events (histogram).

in Table I. The estimated number of background events is equal to 0.9. The systematic uncertainty of background calculation is taken to be 100%.

The spectrum of the $\eta\pi^0$ invariant mass ($M_{\eta\pi^0}$) for $e^+e^- \rightarrow \omega\eta\pi^0$ candidate events is shown in Fig. 4. The π^0 candidate with the maximal difference $|M_{\pi^0\gamma} - M_\omega|$ is used to calculate $M_{\eta\pi^0}$. For comparison, we also show the spectra for the simulated events of the process $e^+e^- \rightarrow \omega a_0(980)$ with the decay $a_0(980) \rightarrow \eta\pi^0$ and of the process $e^+e^- \rightarrow \omega\eta\pi^0$ with uniform phase-space distribution of the final particles. It is evident that the data $M_{\eta\pi^0}$ spectrum is consistent with the distribution for the $\omega a_0(980)$ model.

IV. DETECTION EFFICIENCY

The detection efficiency for the events of the process $e^+e^- \rightarrow \omega a_0(980) \rightarrow \omega\eta\pi^0 \rightarrow \eta\pi^0\pi^0\gamma \rightarrow 7\gamma$ is determined using MC simulation. The simulation takes into account the initial state radiative corrections [11], in particular, the emission of additional photons.

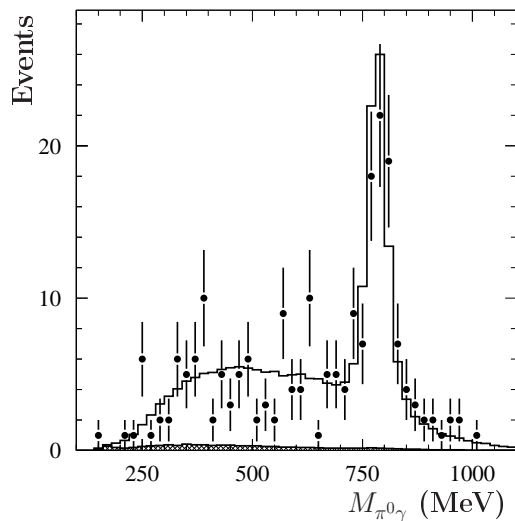


FIG. 3: The $M_{\pi^0\gamma}$ spectrum for selected $e^+e^- \rightarrow \eta 2\pi^0\gamma$ candidate events (points with error bars, two entries per event). The histogram is the sum of the distributions for simulated $e^+e^- \rightarrow \omega\eta\pi^0$ and background events. The simulated distribution is normalized to the number of data events. The shaded histogram shows the background distribution.

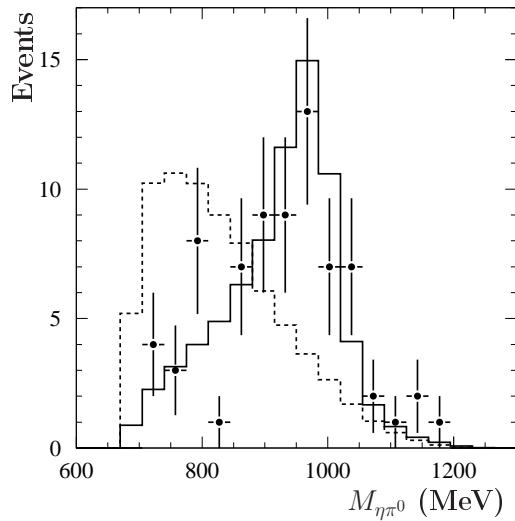


FIG. 4: The $M_{\eta\pi^0}$ spectrum for selected $e^+e^- \rightarrow \omega\eta\pi^0$ candidate events (points with error bars). The solid histogram represents $e^+e^- \rightarrow \omega a_0(980)$ simulation, while the dashed histogram represents simulation of the process $e^+e^- \rightarrow \omega\eta\pi^0$ with uniform phase-space distribution of the final particles.

The detection efficiency ϵ_r is determined as a function of two parameters: the c.m. energy \sqrt{s} and the energy of the additional photon E_r emitted from the initial state. Figure 5 shows the dependence of the detection efficiency on E_r for three representative c.m. energies. The values of the detection efficiency at $E_r = 0$ averaged over the energy intervals are given in Table I.

To estimate the systematic uncertainty of the detection efficiency determination, we use the results of Ref. [2] where the difference in the detector responses between data and simulation for seven-photon events was studied. Based on this study, the systematic uncertainty on the detection efficiency is estimated to be 3%.

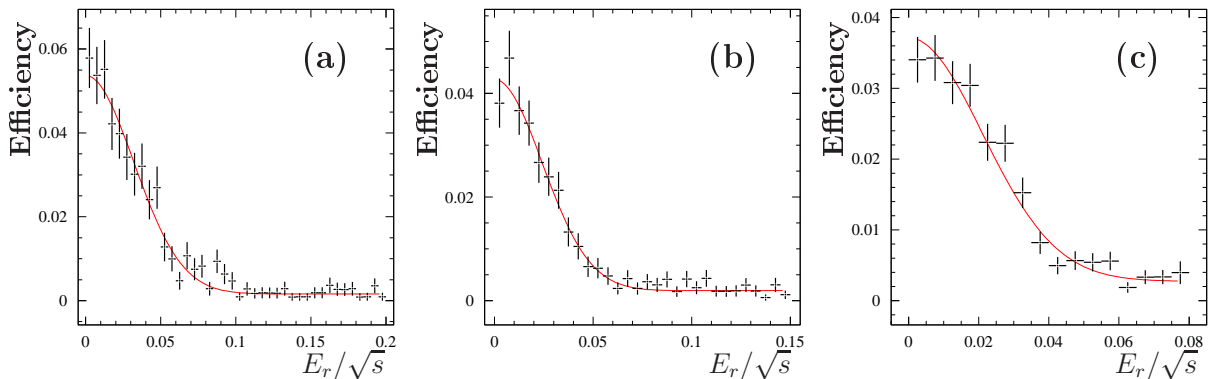


FIG. 5: The dependence of the detection efficiency for $e^+e^- \rightarrow \omega a_0(980) \rightarrow \omega \eta \pi^0 \rightarrow \eta \pi^0 \pi^0 \gamma \rightarrow 7\gamma$ events on the energy of the additional photon emitted from the initial state for $\sqrt{s} = 2.0$ GeV (a), 1.76 GeV (b) and 1.6 GeV (c). The points with error bars are obtained from simulation. The curve shows the result of approximation of the $\epsilon_r(\sqrt{s}, E_r)$ dependence by a smooth function.

V. BORN CROSS SECTION FOR THE REACTION $e^+e^- \rightarrow \omega \eta \pi^0$

The visible cross section for the process $e^+e^- \rightarrow \omega \eta \pi^0$ is related to the Born cross section ($\sigma(E)$) by the following formula:

$$\sigma_{vis}(s) = B \int_0^{x_{max}} \epsilon_r(\sqrt{s}, \frac{x\sqrt{s}}{2}) F(s, x) \sigma(s(1-x)) dx, \quad (2)$$

where $F(s, x)$ is the so called radiator function describing the probability of radiating a certain energy fraction $x = 2E_r/\sqrt{s}$ carried away by photons emitted from the initial state [11], and B is a product of branching fractions $B = \mathcal{B}(\omega \rightarrow \pi^0 \gamma) \mathcal{B}(\eta \rightarrow \gamma \gamma) \mathcal{B}(\pi^0 \rightarrow \gamma \gamma) \mathcal{B}(\pi^0 \rightarrow \gamma \gamma)$ [5]. Equation (2) can be rewritten in the conventional form:

$$\sigma_{vis}(s) = \sigma(s) B \epsilon(\sqrt{s}) (1 + \delta(s)), \quad (3)$$

where the detection efficiency $\epsilon(\sqrt{s})$ and the radiative correction $\delta(s)$ are defined as follows:

$$\epsilon(\sqrt{s}) \equiv \epsilon_r(\sqrt{s}, 0), \quad (4)$$

$$\delta(s) = \frac{\int_0^{x_{max}} \epsilon_r(\sqrt{s}, \frac{x\sqrt{s}}{2}) F(s, x) \sigma(s(1-x)) dx}{\epsilon_r(\sqrt{s}, 0) \sigma(s)} - 1. \quad (5)$$

Technically the experimental Born cross section is determined as follows. Using Eq. (2), the energy dependence of the measured visible cross section $\sigma_{vis,i} = (N_i - N_{bkg,i})/L_i$ is fitted by a theoretical model that describes data reasonably well. Here N_i , $N_{bkg,i}$, and L_i are respectively the number of selected data events, the number of background events, and the integrated luminosity for the i -th energy interval. The fitted parameters of the theoretical model are used to calculate the radiative corrections. Then the experimental Born cross section σ_i is calculated using Eq.(3).

The energy dependence of the Born cross section for the process $e^+e^- \rightarrow \omega \eta \pi^0$ is parametrized according to the vector meson dominance model [18] assuming the $\omega a_0(980)$ intermediate state mechanism. The cross section is described by the contribution of only one resonance with the mass m_V and width Γ_V :

$$\sigma(s) = \sigma_V \frac{m_V^3 q(s)}{s^{3/2} q(m_V^2)} \frac{m_V^2 \Gamma_V^2}{(m_V^2 - s)^2 + s \Gamma_V^2}, \quad (6)$$

where σ_V is the cross section at $s = m_V^2$ and the function $q(s)$ describes the energy dependence of the phase space volume of the final state. Far away from the threshold of the reaction $e^+e^- \rightarrow \omega a_0(980)$, when we can neglect finite widths of the ω and $a_0(980)$ resonances, $q(s)$ coincides with the $a_0(980)$ momentum.

Free fit parameters are σ_V , M_V , and Γ_V . The resulting curve is shown in Fig. 6 along with the values of the Born cross section calculated according to Eq.(3). The obtained values of the mass and width of the resonance,

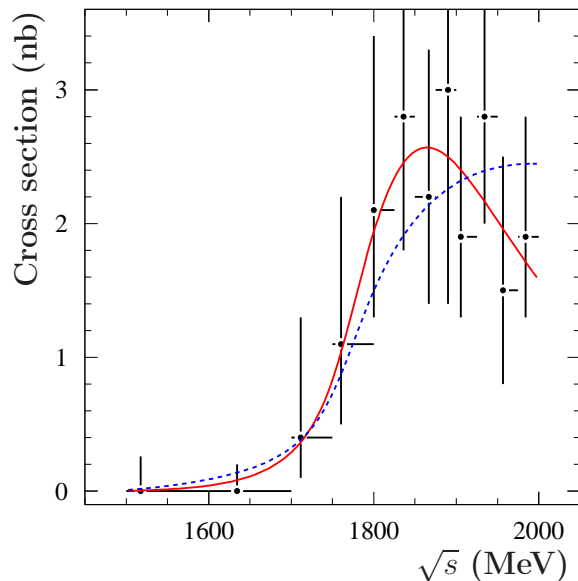


FIG. 6: The cross section for the process $e^+e^- \rightarrow \omega\eta\pi^0$ measured in this work. The solid (dashed) curve shows the result of the fit with (without) a resonance contribution.

TABLE I: The energy interval, integrated luminosity (L), number of selected events (N), estimated number of background events (N_{bkg}), detection efficiency for $e^+e^- \rightarrow \omega\eta\pi^0 \rightarrow 7\gamma$ events (ϵ), radiative correction ($\delta + 1$), and $e^+e^- \rightarrow \omega\eta\pi^0$ Born cross section (σ). The shown cross-section errors are statistical. The systematic error is 4.2%. The 90% confidence level upper limits are listed for the first two energy intervals.

\sqrt{s} (MeV)	L (nb $^{-1}$)	N	N_{bkg}	ϵ (%)	$\delta + 1$	σ (nb)
1500 \div 1600	5888	0	0.02	2.85	0.779	< 0.26
1600 \div 1700	5004	0	0.21	4.03	0.815	< 0.20
1700 \div 1750	2261	1	0.13	4.25	0.813	$0.4^{+0.9}_{-0.3}$
1750 \div 1800	2392	3	0.09	4.29	0.810	$1.1^{+1.1}_{-0.6}$
1800 \div 1825	2373	6	0.09	4.61	0.823	$2.1^{+1.3}_{-0.8}$
1825 \div 1850	1897	7	0.05	5.02	0.841	$2.8^{+1.5}_{-1.0}$
1850 \div 1875	2527	8	0.06	5.34	0.855	$2.2^{+1.1}_{-0.8}$
1875 \div 1900	662	3	0.02	5.58	0.865	$3.0^{+2.9}_{-1.6}$
1900 \div 1925	3459	9	0.07	5.12	0.871	$1.9^{+0.9}_{-0.6}$
1925 \div 1950	2361	11	0.05	5.98	0.880	$2.8^{+1.1}_{-0.8}$
1950 \div 1975	2077	5	0.06	5.64	0.887	$1.5^{+1.0}_{-0.7}$
1975 \div 2000	2682	9	0.06	6.14	0.893	$1.9^{+0.9}_{-0.6}$

$M_V = 1815_{-118}^{+44}$ MeV and $\Gamma_V = 349_{-118}^{+393}$ MeV, are statistically consistent with the $\rho(1700)$ -resonance parameters [5]. We also perform a phase-space fit without a resonance contribution [$\Gamma_V \rightarrow \infty$ in Eq. (6)]. The fit shown in Fig. 6 by the dashed curve also describes data well. The significance of the resonance contribution estimated from the difference of the logarithmic likelihoods of the fits with and without resonance is about 1.2σ .

The numerical values of the Born cross section and radiative corrections are listed in Table I. The total systematic uncertainty on the cross section is 4.2%. It includes the systematic uncertainties on the detection efficiency (3%), luminosity measurement (2.2%), and radiative correction (2%). The latter is estimated by varying the fit parameters within their errors.

VI. CONCLUSION

We have analyzed data collected in the experiment with the SND detector at the e^+e^- collider VEPP-2000 in the c.m. energy range from 1.05 to 2.00 GeV. In the seven-photon final state, events of the process $e^+e^- \rightarrow \eta\pi^0\pi^0\gamma$ have been separated. Most of these events come from the process $e^+e^- \rightarrow \omega\eta\pi^0$. We have measured the cross section for this process for the first time. It has a threshold at 1.75 GeV. The cross section value in the energy range 1.8-2.0 GeV is about 2 nb, approximately 5% of the total hadronic cross section in this energy range. From the analysis of the $\eta\pi^0$ invariant mass spectrum, it has been found that the dominant mechanism of the reaction $e^+e^- \rightarrow \eta\pi^0\pi^0\gamma$ is the $\omega a_0(980)$ intermediate state.

VII. ACKNOWLEDGMENTS

Part of this work related to the photon reconstruction algorithm in the electromagnetic calorimeter for multiphoton events is supported by the Russian Science Foundation (project No. 14-50-00080).

-
- [1] M. N. Achasov *et al.* (SND Collaboration), Phys. Rev. D **88**, 054013 (2013)
 - [2] M. N. Achasov *et al.* (SND Collaboration), Phys. Rev. D **90**, 032002 (2014).
 - [3] M. N. Achasov *et al.* (SND Collaboration), Phys. Rev. D **91**, 092010 (2015)
 - [4] M. N. Achasov *et al.* (SND Collaboration), JETP Lett. **102**, 266 (2015).
 - [5] K. A. Olive *et al.* (Particle Data Group), Chin. Phys. C, **38**, 090001 (2014).
 - [6] A. Romanov *et al.*, in *Proceedings of Particle Accelerator Conference PAC 2013, Pasadena, CA USA, 2013*, p.14.
 - [7] M. N. Achasov *et al.*, Nucl. Instrum. Methods Phys. Res., Sect. A **598**, 31 (2009).
 - [8] V. M. Aulchenko *et al.*, Nucl. Instrum. Methods Phys. Res., Sect. A **598**, 102 (2009).
 - [9] A. Y. Barnyakov *et al.*, JINST **9**, C09023 (2014); A. Y. Barnyakov *et al.*, Instrum. Exp. Tech. **58**, 30 (2015).
 - [10] V. M. Aulchenko *et al.*, Nucl. Instrum. Methods Phys. Res., Sect. A **598**, 340 (2009).
 - [11] E. A. Kuraev and V. S. Fadin, Yad. Fiz. **41**, 733 (1985) [Sov. J. Nucl. Phys. **41**, 466 (1985)].
 - [12] G. Bonneau and F. Martin, Nucl. Phys. **B27**, 381 (1971).
 - [13] S. Agostinelli *et al.*, Nucl. Instrum. Methods Phys. Res., Sect. A **506**, 250 (2003).
 - [14] A. V. Bozhenok, V. N. Ivanchenko, Z. K. Silagadze, Nucl. Instrum. Methods Phys. Res., Sect. A **379**, 507 (1996).
 - [15] B. Aubert *et al.* (BABAR Collaboration), Phys. Rev. D **73**, 052003 (2006).
 - [16] B. Aubert *et al.* (BABAR Collaboration), Phys. Rev. D **76**, 092005 (2007); **77**, 119902(E) (2008).
 - [17] B. Aubert *et al.* (BABAR Collaboration), Phys. Rev. D **77**, 092002 (2008).
 - [18] N. N. Achasov and A. A. Kozhevnikov, Phys. Rev. D **55**, 2663 (1997).